Anal. Chem. **2004**, *76*, 1773−1777

Mass Transfer and Gas-Phase Calibration of Implanted Oxygen Sensors

Milan T. Makale, Michael C. Jablecki, and David A. Gough*,†

Department of Bioengineering, University of California San Diego, La Jolla, California 92093

A protocol is described for validation of implanted oxygen sensors, in which sensors are calibrated in the gas phase where concentration boundary layers are absent. Calibration prior to sensor implantation and confirmation after sensor explantation allows separation of tissue mass transfer effects from sensor variance and drift. A model is given here that describes the oxygen-dependent signal current in terms of oxygen mass transfer to the sensor, permeability of the sensor membrane, and electrode area. The parameter used in the model to describe mass transfer to implanted sensors is consistent with experimental observations and allows comparisons with nonimplanted sensors. This method provides a bridge between the complementary approaches of empirical calibration and model-based calculation for determining oxygen concentration from the sensor response.

Conventional membrane-covered oxygen electrode sensors used in biological applications function by electrochemical consumption of oxygen.[1] Oxygen arrives at the outer hydrophobic membrane of the sensor by convective and diffusive mass transfer, then partitions into the membrane and diffuses to the electrode surface, where quantitative electrochemical reduction of oxygen occurs with the simultaneous production of the signal current. For a given concentration of oxygen in the well-mixed bulk, there is a relationship (given explicitly below) between the overall mass transfer of oxygen to the sensor, the permeability of the sensor membrane, the electrode area, and the signal current. Quantitative oxygen sensing can be achieved using this relationship to *calculate* the oxygen concentration from current measurements when the active electrode area of the sensor and membrane permeability are specified, the overall mass transfer is quantified and constant, and bulk oxygen concentration is the only variable.

This calculation approach is, however, rarely used in oxygen monitoring because it is often more convenient to employ a simple *calibration* approach based on an observed correlation between the signal and bulk oxygen concentration. Using the calibration approach, an empirical proportionality relationship is first established between the concentration and signal by recording signals from standards of known oxygen concentration under specified mass transfer conditions. This relationship is then applied to the sensor signal obtained in the measurement process to infer oxygen concentration.

The tacit requirement for employing a calibration approach in a completely quantitative way is that identical mass transfer conditions must prevail between the calibration procedure and the measurement process. This requirement can sometimes be met for measurements made in the liquid phase, in which calibration solutions and the assay medium have very similar properties and can be comparably stirred. However, the requirement for identical mass transfer conditions is not easily met when the sensor is employed as an implant in biological tissues, because the sensor is usually calibrated prior to implantation in well-stirred solutions, but the measurement takes place in heterogeneous tissues. In this situation, the reported concentration of oxygen differs from the actual tissue concentration in proportion to the difference in mass transfer between the two media, which is usually not accurately known but may be substantial. Measurements of this type in tissues report only relative steady-state values and temporal changes in oxygen, which may be sufficient in some cases,[2,3] but are inadequate for certain purposes. To equate calibration-based values of oxygen to model-based calculated values, it is necessary to establish a sensor calibration procedure that accounts for differences in mass transfer between the calibration conditions and actual measurement conditions.

There are additional considerations when a sensor is used as an implant. Several investigators have observed that identical implanted sensors can occasionally produce quite different responses, for example, one signal rising and the other simultaneously falling, to a given concentration challenge. There are two general explanations for such differences. First, the sensitivity of the sensor itself may have changed during use or may have been altered by implantation. To test this hypothesis, it is necessary to compare sensor sensitivity before implantation and after explantation under identical conditions. If only minor differences are observed, the differential responses are likely due to other factors. An alternative explanation is related to the intrinsic properties of tissues, namely, there may exist a distribution of oxygen in tissues. It is well-documented that oxygen concentration in tissues is heterogeneous on the scale of intercapillary distances (10−100 μm) (e.g., see refs 3, 4), but there is little evidence for heterogeneity at other scales. Oxygen distributions can be attributed to local

* Corresponding author address: Department of Bioengineering, University of California San Diego, 9500 Gilman Drive, La Jolla, CA 92093-0412. Phone: 858-822−3446. Fax: 858-534-5722. E-mail: dgough@bioeng.ucsd.edu.

† D.A.G. is a scientific advisor to GlySens, Inc.

(1) Fatt, I. *Polarographic Oxygen Sensors*; CRC Press: Cleveland, OH, 1976.

(2) Clark, L. C., Jr. *Trans. ASAIO* **1956**, *2*, 41−48.

(3) *Oxygen Transport to Tissue*; Andreas, E.; Delpy, D. T., Eds.; Klumer Academic/Plenum Publishers: New York, NY, 1999; XXI.

(4) Dewhirst, M. W.; Klitzman, B.; Braun, R. D.; Brizewl, D.; Haroon, Z. A.; Secomb, T. W. *Int. J. Cancer* **2000**, *90*, 237−255.

10.1021/ac0352169 CCC: $27.50
Published on Web 02/12/2004

differences in microvascular patterns, blood oxygen concentration, or differences in mass transfer resistance.

In this communication, we describe a study in which independently connected oxygen sensors in an array are calibrated in the gas phase and implanted for several weeks in a novel hamster window chamber preparation to record tissue oxygen, and the calibration is confirmed after explantation. Gas-phase calibration provides repeatable conditions in which external boundary layers are absent and the stability of individual sensors can be unequivocally determined. A comparison of the calibrated response in the gas phase to the observed response when implanted and an assumption of uniform blood oxygen concentration provide a basis for estimation of a specific mass transfer coefficient for each implanted sensor. This information may be useful to understand the response of implanted sensors and to guide the design of new sensors. A model of the sensor signal current that incorporates these considerations is proposed.

THEORETICAL

The model is cast in terms of oxygen mass transfer to a disk electrode covered with a hydrophobic membrane. Mass transfer to a given sensor from the homogeneous bulk is described by a mass transfer coefficient characteristic of the stirring conditions and properties of the medium. The boundary conditions are zero concentration at the electrode surface due to quantitative electrochemical consumption, matched fluxes at the membrane-tissue interface, and specified homogeneous bulk concentration far from the sensor surface in calibration experiments or specified inspired gas concentration in animal experiments. The model assumes one-dimensional diffusion normal to the electrode surface and is applicable when the electrode diameter is much larger than the overall membrane thickness. The model is a variant of one proposed previously.[5]

The steady-state solution for the oxygen-dependent current $i_{o,i}$ is

$$i_{o,i} = \frac{nFAP_m c_o}{(1 + Bi_i^{-1})} \quad (1)$$

where n is the electron equivalent, F is the Faraday constant, A is the electrode area, c_o is the bulk oxygen concentration, and P_m is the membrane permeability given by $P_m = \alpha D_m/\delta_m$, in which α is the equilibrium partition coefficient, D_m is the diffusion coefficient for oxygen in the membrane, and δ_m is membrane thickness. Bi_i is the dimensionless ratio of external to internal mass transfer given by $Bi_i = h_i/P_m$, where h_i is an external mass transfer coefficient. The index i indicates the medium in which the measurement is made, and can be set at g, l, or t, corresponding to the gas phase, liquid phase or tissue, respectively.

The mass transfer parameter h_i is used to describe the overall rate of external mass transfer, regardless of the particular mass transfer mechanisms involved. For example, in stirred liquid medium, external mass transfer occurs by oxygen diffusion within a relatively stagnant liquid layer adjacent to the sensor. Under these conditions, the mass transfer parameter is given by $h_l = D_l/\delta_l$, where D_l is the diffusion coefficient of oxygen in the stagnant liquid at the interface and δ_l is the nominal concentration boundary layer thickness or diffusional distance. In the gas phase where boundary layers are insignificant, external mass transfer is much more rapid than diffusion within the membrane, and $Bi_g \rightarrow \infty$. Here, the gas-phase signal current, $i_{o,g}$, is limited by diffusion within the membrane, and $i_{o,g} \rightarrow nFAP_m c_o$, allowing estimation of P_m. For implanted sensors, the overall mass transfer process can be described by a series of mechanisms, including oxygen inspiration, pulmonary exchange, complexation with hemoglobin, conveyance via blood circulation to the local tissue, and diffusion from nearby microvasculature to the sensor surface, the slowest step of which can be considered the limiting mass transfer resistance.

Equation 1 can be rearranged as follows to give the external mass transfer coefficient.

$$h_i = \frac{P_m i_{o,i}}{nFAP_m c_o - i_{o,i}} \quad (2)$$

With measurements of the steady-state current, $i_{o,i}$, the external mass transfer parameter, h_i, can be estimated from independently determined values of A, P_m (from gas-phase measurements), and the steady-state concentration, c_o. For measurements in a stirred liquid or stagnant tissue, and when the external diffusion coefficient, D_i, is known from an independent source, the effective diffusional distance, δ_i, can be estimated.

METHODS

Sensor Fabrication. A disk-shaped sensor array containing 18 platinum working electrodes, several counter electrodes, and a common Ag/AgCl potential reference electrode was fabricated by thick-film deposition of electrode materials onto an alumina substrate.[6] Individual working electrodes were either 125 or 300 μm in diameter and were separated by a minimum of 3000 μm. The disk was covered by a 10-μm layer of conductive electrolyte (1.0 N NaCl, pH 7.3, in cross-linked poly(hydroxyethyl methacrylate) gel) and a 25-μm layer of spin-cast poly(dimethylsiloxane). Electrodes were connected to a multichannel potentiostat, and data were archived by computer. Because it was difficult to avoid electrical short circuits in the connector junctions at current levels obtained in these studies ($\sim 10^{-9}$ amp), every effort was made to minimize manipulation of the connectors. Further details of the sensor array design fabrication process are given elsewhere.[6]

Sensor Characterization. Sensors were individually characterized before and after the implantation experiment. The response of a given sensor was compared only with that of the same sensor under different measurement conditions, and no attempt was made to average signals from multiple sensors for purposes of oxygen determination. This approach provided a basis of evaluating the stability of individual sensors without limitations due to the reproducibility of sensor fabrication.

Sensors were first characterized in the gas phase to provide quantitative values for P_m without boundary layer effects. Oxygen concentrations in the gas phase were based on analyzed mixed gases, corrected for barometric pressure and humidity. It was important to humidify the gas to saturation levels to avoid drying out the electrolyte layer of the sensor. Electrode area and

(5) Leypoldt, J. K.; Gough, D. A. *Anal. Chem.* **1984**, *56*, 2896–2904.

(6) Makale, M.; Lin, J. T.; Calou, R.; Tsai, A.; Chen, P.; Gough, D. A. *Am. J. Physiol.* **2003**, *284*, H2288–H2294.

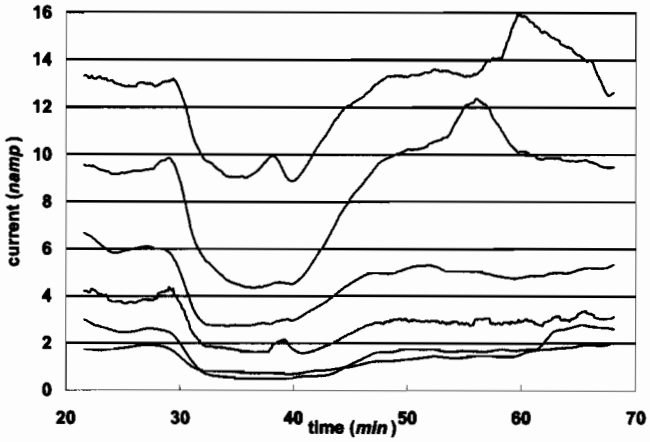

Figure 1. Example of responses of implanted sensors. Inspired oxygen concentration went from atmospheric (20.9%) to 10.0% at 30 min and back to atmospheric at 40 min.

membrane thickness were estimated by microscopic examination. For comparison, repeatable stirring conditions were employed in liquid-phase experiments to obtain boundary layer conditions that were as reproducible as possible, although obtaining a uniform boundary layer thickness at all points on the array surface was unlikely. All studies were carried out at 37 °C.

Sensor Array Implants in Tissue. Sensor arrays were implanted in a hamster window chamber preparation contacting subcutaneous connective tissues.[6] This implant preparation allows repetitive and nondestructive microscopic imaging of the tissue adjacent to individual sensors without the depressive effects of anesthesia while simultaneously recording sensor signals. Tissue oxygen challenges were created by abruptly changing the inspired gas between atmospheric (20.9%) and hypoxic (10.0 or 15%) oxygen levels. Sensors remained functional as implants for over 2 months in some cases. Details of the implantation and tissue imaging procedures are given elsewhere.[6]

RESULTS AND DISCUSSION

The results selected here are typical of data from a larger pool.

Mass Transfer to Implanted Sensors. Figure 1 is an example of the response of several sensors on a selected implanted array to abrupt oxygen changes in the inspired gas. These results were obtained on day 7 after implantation in a hamster window chamber. All sensors produced lower signals when implanted, as compared to gas-phase values. Implanted sensors also demonstrated a range of steady-state signal amplitudes, including relatively low to high signals. The signal changes shown were approximately linear with inspired oxygen concentration changes, but linearity was not universally the case. For the majority of sensors that retained sensitivity to oxygen at the post-explant calibration verification, the differences in signal amplitude as implants are likely due to small differences in local tissue structure. The signals also show a characteristic temporal variation, not to be confused with noise, due to local tissue autoregulation of perfusion. Although most sensors showed a consistent transient response to the oxygen challenge, the response to the downward concentration change was always rapid compared to that to the upward change. These observations demonstrate the importance of post-explantation calibration under repeatable conditions for resolving effects of the tissue environment from intrinsic sensor properties.

Table 1. Examples of Sensor Sensitivity in the Gas Phase and Implanted[a]

	i_o/Ac_o (amp·cm·mole^{-1}) × 10^3			
sensor ID	preimplant	postexplant	pre- minus post-	implanted (day 20)
10−4	152.0	130.0	22.1 (17.0%)	4.9 (3.8%)
10−5	84.2	98.9	−14.7 (−14.7%)	4.3 (4.3%)
10−7	127.0	106.3	20.7 (19.4%)	5.9 (5.6%)
10−9	121.1	125.5	−4.5 (−3.6%)	11.4 (9.1%)
10−13	157.8	141.0	16.8 (11.9%)	7.1 (5.0%)
10−16	119.6	110.4	9.2 (8.3%)	10.6 (9.6%)
$\bar{X}$	127.0	118.7	14.7 (12.5%)	7.4 (6.2%)
SD	26.4	16.0	2.8 (2.4%)	1.21 (1.0%)
SD/$\bar{X}$	0.21	0.14	0.19 (0.19)	0.41 (0.41)

[a] *t*-Test result: preimplant vs postexplant is not significantly different.

Gas-Phase Characterization. Examples of sensor characterization results are shown in Table 1. The table contains values of the specific current density, i_o/Ac_o, determined in the gas phase for selected sensors before implantation and after explantation, their differences, and as implanted at day 20. The reported values are averages of three successive steady-state values for each sensor under the indicated conditions. Given in parentheses are the percentage differences between preimplant and postexplant, and between implant and postexplant. The mean, standard deviation, and ratio of the standard deviation to the mean are also given. Offset currents in the absence of oxygen were estimated to be $<0.3 \times 10^{-9}$ amp by linear regression of current against concentration and were subtracted.

Although the majority of sensors remained responsive to oxygen during the entire study, ~10% of sensors (not included here) had electrical connection failures. These sensors produced predictable oxygen-dependent currents at the preimplant calibration, but later failed by producing near-zero, oxygen-insensitive currents either during the implant phase or during postexplant characterization. Most electrical contact failures occurred at the connection between the sensor and cable strip to the multichannel potentiostat. It is surprisingly difficult to maintain fully reliable electrical connections at the nanoamp current level when the connectors are frequently manipulated, as was necessary in this study. Connector problems can be addressed at a later stage when sensors are fabricated for clinical application with permanent connections.

After an initial signal stabilization period, there was no systematic change in sensitivity with time in the vast majority of sensors. Most sensors produced either slightly lower or higher specific current density after explantation compared to the preimplant calibration, although there were no systematic differences in either direction. The mean difference and standard deviation between preimplant and postexplant were 12.5 and ±2.4%, respectively. One possible explanation for these differences is modification of the thickness of the membrane or electrolyte layer due to mechanical forces at implantation, during operation as an implant, or at explantation. No evidence was found for the extraction of membrane material by phagocytic cells or the deposition of a proteinaceous coating on the membrane.

Implanted sensors showed several differences from their in vitro performance. Most prominent, the mean specific current

Table 2. Example of Membrane Properties Determined in the Gas Phase[a]

P_m(cm·s^{-1}) × 10^4	δ_m(cm) × 10^4	αD_m(cm^2·s^{-1}) × 10^5
64.5 ±.0.9	49.0 ± 0.4	3.2 ± 0.1

[a] Value ± estimated error.

density during the implant phase was substantially lower than the preimplant mean, the postexplant mean, and the pre- minus post-difference mean, reflecting the larger mass transfer resistance of tissues. Although sensors having different nominal electrode area were included in the table (but not distinguished), there was little effect of electrode area on the specific current density in vitro, suggesting that the one-dimensional diffusion model was justified. More data are needed to determine if the specific current density is strictly independent of electrode area in vivo.

The implant signal standard deviation was much smaller than the respective in vitro standard deviation, corresponding to the lower implant signal mean. However, the normalized standard deviation, or the standard deviation scaled by the mean, was substantially larger for the implanted sensors (0.41), compared to preimplant (0.21), postexplant (0.14), and the pre- minus post-difference (0.19). The rankings of individual sensor signal magnitude were also not conserved from in vitro to in vivo recordings. These observations suggest that factors producing a greater range of signal variance are present when a sensor is operated as an implant. These factors may include (1) the nonuniform distribution of microscopic blood vessels[3,4] within tissues adjacent to individual sensors and (2) variations in tissue composition and permeability to oxygen, resulting in local differences in mass transfer resistance. Other determinants of the overall oxygen mass transfer, such as gas exchange in the airways and convection within major blood vessels to the implant site, are expected to have a common effect on sensors located at a given tissue site. Heterogeneity within tissues on a scale that is large compared to sensor size has been a key reason for the ambiguous responses of individual implanted sensors in the past. Some properties of tissues that affect sensor signals have been analyzed in detail elsewhere.[4,6]

Membrane Parameters. An example of determination of sensor membrane permeability and related parameters from a gas-phase experiment is given in Table 2. The table includes the permeability determined from eq 1 with $Bi_g \rightarrow \infty$, the membrane thickness estimated by optical microscopy, and the product of the solubility and diffusivity of oxygen, αD_m. Using typical values for the solubility of oxygen in silicone rubber from the literature,[7] the value for the diffusivity is consistent with previously published values.[8]

To assess the effect of the internal electrolyte layer on mass transfer, the permeability of internal electrolyte layers of hypothetical thicknesses was compared to the permeability of the membrane. As long as the electrolyte layer was comparable to or thinner than the silicone rubber membrane, the internal liquid layer had little effect. In certain early sensor arrays, however, the membrane became obviously convex due to slow osmotic exchange from the external solution, and the internal solution did not remain uniformly thin across the electrode surface, leading to a predictable pattern of sensitivity variability to oxygen across the disk. This was avoided in later fabrications by the use of a small deposit of adhesive near the center of the disk to fix the membrane and ensure specified liquid layer spacing.

Table 3. Examples of Mass Transfer in the Stirred Liquid Phase[a]

sensor ID	$i_{o,l}$(amp) × 10^9	Bi_l	h_l(cm·s^{-1}) × 10^4	δ_l(cm) × 10^4
7−1	15.2	0.67	43.0	a
7−2	15.3	0.51	38.4	59.9
7−3	14.1	0.50	37.7	66.4
$\bar{X}$	14.9	0.56	39.7	60.0

[a] $c_o = 22.0 \times 10^{-8}$ mol·cm^{-3}, $D_l = 2.3 \times 10^{-5}$ cm^2·s^{-1}.

Table 4. Examples of Mass Transfer in Tissues

sensor ID	$i_{o,t}$(amp) × 10^9	c_o(mol·cm^{-3}) × 10^8	Bi_t	h_t(cm·s^{-1}) × 10^4
4−1	11.3	22.0	0.031	1.99
4−2	7.29	as above	0.019	1.21
4−3	5.66	as above	0.016	1.03
4−1	10.1	15.8	0.038	2.50
4−2	5.83	as above	0.021	1.35
4−3	3.96	as above	0.016	1.01

Mass Transfer Parameters in the Stirred Liquid Phase. For comparison, examples of mass transfer in the well-stirred liquid phase are shown in Table 3, on the basis of permeability values determined previously in the gas phase and values for oxygen diffusivity in the liquid phase from the literature.[5] In this example, an effort was made to obtain consistent stirring conditions, and the external concentration boundary layer thickness ranged from ~54 to 66 μm. These dimensions are consistent with expectations under these conditions where the mass diffusivity is much lower than the kinematic viscosity, and the concentration boundary layer is strongly dependent on stirring.[9] We note that it is difficult to achieve consistent stirring conditions that are uniform across the array, which is important for analyzing the response to rapidly diffusing molecules such as oxygen.

Justification for the Mass Transfer Parameter Used in Tissues. It is clear that a lumped parameter such as h_l can be effective to represent mass transfer in the homogeneous liquid phase, but application of the analogous parameter in tissues may not be so obvious. To reach implanted sensors, oxygen follows a pathway from the well-mixed atmosphere that includes several steps, namely, convection through pulmonary airways, exchange into the arterial blood, convection by the systemic circulation to the tissue region in which the sensor array is implanted, transit through tissues via the microcirculation, and diffusion to the sensor. In the model used here, the predominant mass transfer resistance is at the point of the largest difference between two segments of the serial pathway. The observations that implanted sensors respond immediately to changes in inspired oxygen and that regional blood flow has a substantial effect on the sensor signal suggest that overall convection to the region of the sensor

(7) Crank, J.; Park, G. S. *Diffusion in Polymers*; Academic Press: London, 1968.
(8) Lucisano, J. Y.; Armor, J. C.; Gough, D. A. *Anal. Chem.* **1987**, *59*, 736−739.
(9) Leal, L. G. *Laminar Flow and Convective Transport Processes*; Butterworth-Heinemann: Boston, MA, 1992.

is a relatively rapid process and that diffusion from there to the sensor surface is the slower, rate-determining step, which is described by h_t. The tissue directly in front of individual sensors is where the largest mass transfer resistance occurs, and this region can extend for various distances in front of respective sensors, depending on microvascular proximity. This situation is analogous to mass transfer in stirred liquid phase, where convective mass transfer occurs mainly external to the boundary layer and diffusion occurs within the boundary layer. The alternative to the present averaged mass transfer parameter, namely, a parameter incorporating detailed mass transfer resistances for individual tissue components, would be difficult to create with available information, would likely have no more general applicability than the averaged parameter, and does not seem necessary for the purpose at hand. The present model is consistent with the clinical mandate to relate tissue oxygenation as indicated by implanted sensor signals to inspired oxygen, which can be adjusted to address therapeutic needs.

To be consistent with this analogy, the mass transfer regime must remain constant and independent of concentration, which is clearly not the case when blood flow to the region or breathing rate are disturbed and become limiting. Therefore, only modest hypoxia challenges were employed to avoid changes in vascular blood flow due to compensatory physiologic mechanisms. In studies (not shown) involving greater inspired oxygen differences, a concentration dependence was observed at the lowest values, suggesting physiologic effects, such as local vasodilation, changes in breathing rate, and circulatory changes. It is difficult to obtain a reproducible tissue perfusion or convective mass transfer regime under these conditions, and alternative models may be more appropriate.

It is intriguing that changes in inspired oxygen concentration can be readily detected by sensors implanted in tissues, even though autoregulatory mechanisms are thought to function within tissues by adjusting local perfusion to maintain constant homeostatic oxygen levels. This process (known as vasomotion) may be most obvious on the dimensional scale of the capillary bed, or several hundred micrometers. The relatively large electrodes used here draw oxygen from multiple capillary beds and may countermand local autoregulatory mechanisms. The electrode size was dictated by a practical requirement, namely, the amplification of signal using implantable instrumentation, which is difficult to isolate from sources of inductive noise.

Implications for Sensor Design. Observations here suggest that there are different tissue mass transfer values for specific implanted sensors, reflecting small differences in local microvascular and tissue structure.[6] In systems in which the external mass transfer is faster than diffusion within the membrane, the system is expected to be diffusion-limited by the membrane and relatively insensitive to tissue heterogeneity, but the response dynamics will be largely determined by membrane properties. If, as seen here, the membrane is relatively permeable, the properties of the tissue and local heterogeneity can be expected to have the greater effect. This information can be used to recommend membrane designs that reduce the effects of tissue heterogeneity on sensor response while still responding sufficiently rapidly to concentration changes. As to the use of this information for operation of implanted sensors, it may be necessary to develop methods of signal averaging if the goal is to report a single value of oxygen concentration representative of the range found in tissue.

Due to the complexity of the response of implanted sensors, it is essential that sensor stability during the implant application be documented by comparison of preimplant and postexplant characterization. Sensing systems that rely on single electrodes produce steady-state signals that are at best representative of only the tissue directly adjacent to the sensor. It should be appreciated that signals from implanted sensors reflect variables, such as blood flow, that determine oxygen delivery as well as oxygen concentration.

CONCLUSIONS

The model describing sensor signal in terms of oxygen concentration, electrode area, and mass transfer properties provides a means for quantitative determination of oxygen mass transfer. With appropriate configuration, the model can be applied to sensor operation in the gas phase, where boundary layers are absent; in the stirred liquid phase; or in tissues. When validated with preimplant and postexplant calibration, the response of implanted sensors can be definitively ascribed to variations in the biological environment, rather than the inherent properties of individual sensors. Implanted oxygen sensors respond rapidly to oxygen concentration challenges and are affected by regional and local blood flow, suggesting that under certain conditions, the simple mass transfer model proposed here is reasonable.

ACKNOWLEDGMENT

This work was supported by grants from the National Institutes of Health and the Department of Defense.

GLOSSARY

A	electrode area, cm^2
Bi	ratio of external to internal mass transfer, dimensionless
c_o	bulk oxygen concentration, $mole \cdot cm^{-3}$
D	diffusion coefficient in the medium, $cm^2 \cdot s^{-1}$
D_m	diffusion coefficient in the membrane, $cm^2 \cdot s^{-1}$
F	Faraday constant, $amp \cdot s \cdot coul^{-1}$
h	mass transfer coefficient, $cm \cdot s^{-1}$
i_o	oxygen diffusion current, amp
n	electron equivalent, dimensionless
P_m	membrane permeability, $cm \cdot s^{-1}$
α	partition coefficient, dimensionless
δ	nominal external diffusion length, cm
δ_m	membrane thickness, cm

Indices

g	gas phase
l	liquid phase
t	tissue

Received for review October 14, 2003. Accepted January 16, 2004.

AC0352169